Early Postmortem Metabolism and Protease Activation in Fast Glycolytic and Slow Oxidative Bovine Muscles

Patricia M. Ramos[1,2], Mayka R. Pedrão[1,3], Lindsey C. Bell[1], and Tracy L. Scheffler[1]*

[1]Department of Animal Sciences, University of Florida, Gainesville, FL, 32611-0910, USA
[2]Department of Animal Sciences, University of São Paulo, Piracicaba, SP, Brazil
[3]Federal Technological University of Paraná, Londrina, PR, Brazil
*Corresponding author. Email: tscheffler@ufl.edu (Tracy L. Scheffler)

Abstract: Muscle properties and metabolism influence muscle to meat conversion. Fiber type profile impacts glycolytic capacity as well as protein turnover rate *in vivo*. Our objective was to investigate protease content and activation during the early postmortem period using muscles with known divergent metabolism. Samples from *longissimus lumborum* (LL) and *diaphragm* (Dia) were taken from predominantly Angus steer carcasses (n = 6) at 1, 3, and 24 h postmortem and frozen. Myosin heavy chain (MyHC) isoforms, ATP, glycogen, glucose, glucose-6-phosphate (G6P), and lactate concentrations were determined. Procaspase-3, calpain-1, calpastatin, desmin, and troponin-T were assessed by immunodetection. Muscles showed contrasting MyHC profiles, with LL represented primarily by IIx and IIa isoforms (∼88%) whereas Dia contained mostly (80%) type I isoform. Glycogen degradation was more pronounced in LL and coincided with more rapid accumulation of glucose and lactate ($P < 0.01$). Procaspase-3 content was influenced by muscle (m: $P < 0.01$), being greater in Dia. Fragments indicating activation of procaspase-3 postmortem were not detected. Calpain-1 autolysis and intact calpastatin (135 kDa) content were influenced by muscle and time (m × t: $P < 0.01$ and $P < 0.01$, respectively). Calpastatin fragmentation postmortem was not associated with greater procaspase-3 content. In conclusion, fast glycolytic LL displayed faster protease activation and greater proteolysis during the first 24 h postmortem.

Introduction

Proteolysis of muscle cytoskeletal and myofibrillar proteins is the key mechanism influencing tenderization during meat aging. The calpain-calpastatin system is well-recognized as the primary contributor to the postmortem breakdown of muscle proteins, including titin, troponin-T, and desmin (Delgado et al., 2001a; Geesink et al. 2006; Geesink and Koohmaraie, 1999; Koohmaraie and Geesink, 2006; Wright et al., 2018). Although the calpain family consists of several isoforms, calpain-1 and calpain-2 are implicated in meat tenderization. Calpain-1 and -2 isoforms are also known as μ- and m-calpain, respectively, which relates

to their calcium requirement for half-maximal activity; while calpain-1 requires ∼ 5 μM Ca^{2+}, calpain-2 requires 0.3-1.0 mM Ca^{2+} (Goll et al., 2003). Calpastatin is the only known endogenous inhibitor for calpains. Elevated calpastatin levels reduce calpain activity, thereby contributing to diminished proteolysis and tenderization. For instance, callipyge sheep possess higher calpastatin activity in pre-rigor *longissimus* than "normal" sheep, resulting in reduced protein degradation and tougher meat (Delgado et al., 2001b). Moreover, the μ-calpain to calpastatin activity ratio is considered a good predictor for tenderization rate (Koohmaraie, 1996). Caspase proteases have been suggested to contribute to variation in meat tenderness via their role in

calpastatin degradation (Huang et al., 2014), though evidence is limited.

The rate of proteolysis is also associated with inherent muscle characteristics. Muscle properties vary to accomplish diverse functions, and these features are reflected in muscle fiber type characteristics. Muscle fibers are classified according to contractile speed (slow vs. fast), which is largely determined by myosin heavy chain (MyHC) isoform composition; and/or predominant metabolism (oxidative vs. glycolytic). In the living animal, fiber recruitment during activity may dictate protein turnover; motor units of type I and IIa fibers are typically activated more frequently, and higher rates of protein synthesis may be necessary to match the higher use-dependent protein degradation rates in these fibers (Goodman et al., 2011). This is consistent with higher calpain activities observed in oxidative muscles postmortem (Whipple and Koohmaraie, 1992). Fiber types have also been shown to exhibit different susceptibilities to apoptosis and cell death. In mice, the red *gastrocnemius* exhibited higher activities of caspase 3, 8, and 9 compared with the white portion (McMillan and Quadrilatero, 2011). Although this points to oxidative fibers being more prone to proteolysis, evidence from animal models indicates that oxidative skeletal muscle is more protected during ischemia than glycolytic muscle (Charles et al., 2017). Similarly, in postmortem pig *longissimus*, type I fibers displayed slower rates of protein degradation than type IIb (fast/glycolytic) fibers (Muroya et al., 2010).

The rate of postmortem metabolism may help explain differences in proteolysis between fiber types. After exsanguination, muscles attempt to maintain normal conditions, and removal of oxygen supply results in a shift to anaerobic glycolysis. Low pH, along with diminished ATP, limit the ability of the Ca^{2+}-ATPase (SERCA) to pump Ca^{2+} into the sarcoplasmic reticulum to maintain resting sarcoplasmic Ca^{2+} concentration. It is possible that calcium uptake by mitochondria helps limit increases in sarcoplasmic Ca^{2+} early postmortem. The significance of mitochondrial calcium transport is supported by Dang et al. (2020), who showed that inhibition of the mitochondrial calcium uniporter contributed to earlier activation of calpain-1. However, accumulation of considerable amounts of Ca^{2+} in mitochondria contributes to Ca^{2+} overload, cell death, and activation of proteases. Along these lines, fibers with fewer mitochondria may have reduced ability to limit increases in sarcoplasmic Ca^{2+}, and consequently experience Ca^{2+} overload and protease activation earlier postmortem. Mitochondria in glycolytic bovine muscle exhibited a more rapid decline in function and outer membrane integrity compared to oxidative muscle (Ramos et al., 2021). Our objective was to evaluate postmortem metabolism and the activation of protease systems in the fast, glycolytic *longissimus lumborum* (LL) and slow, oxidative *diaphragm* (Dia). We hypothesized that the reduced mitochondrial content in the LL would contribute to hastened early postmortem metabolism and protease activation.

Materials and Methods

Animals and sampling

Primarily Angus (80 to 100% genetics) steers (n = 6) were harvested at approximately 18.5 months and 630 kg live weight at the University of Florida Meat Processing Center, inspected by the United States Department of Agriculture (USDA-FSIS). Sampling was during the summer on 3 slaughter dates (2 animals/day). Samples from LL and Dia muscles were collected at 1, 3, and 24 h postmortem, flash-frozen in liquid nitrogen, and stored in an ultra-low freezer (−80°C) until analysis.

Myosin heavy chain composition

The previously flash-frozen postmortem muscle samples were used to characterize MyHC isoform composition (n = 18 per muscle). Extraction, preparation, and electrophoresis followed Scheffler et al. (2018), with 2 μg of protein loaded per well. Gels were scanned using the Odyssey CLx imaging system (LI-COR Biosciences, Lincoln, NE) and quantified using Image Studio software. The percentages of each myosin heavy chain isoform (I, IIa, IIx) were calculated based on the signal from each specific band relative to total signal.

Muscle substrate and metabolites

Samples from both muscles at all 3 time points (n = 36) were powdered using liquid nitrogen. Protocols used for glycogen, glucose, glucose-6-phosphate (G6P), and lactate content were modified from Copenhafer et al. (2006), which was based on enzymatic analysis methods from Bergmeyer (1974). Briefly, for glycogen, 100 mg powdered muscle was diluted with 1,000 μl 2 M HCl (1:10, w/v) and homogenized using a bead-beating homogenizer (Precellys 24 Homogenizer, Bertin Instruments, Rockville, MD). Homogenate was incubated at 95°C for 2 h to hydrolyze glycogen to glucose units; this was followed by centrifugation at $15,000 \times g$ for 10 min.

The supernatant was transferred to a new tube, neutralized with 2 M NaOH (1:1) and stored (−80°C) until the assay was performed. Samples were plated in duplicate on 96 well plates, followed by addition of assay media (final concentration: 90 mM triethanolamine, 6 mM EDTA, 9 mM $MgCl_2$, 0.5 mM NADP and 1.2 mM ATP, pH adjusted to 7.6). Initial absorbance was determined at 340 nm using a multi-well plate reader (Synergy HT, BioTek Instruments, Winooski, VT). Then, an enzyme cocktail containing hexokinase (HK, 1.5 U/well; Roche; Indianapolis, IN) and glucose-6-phosphate dehydrogenase (G6PDH, 1.3 U/well; Roche; Indianapolis, IN) was added to each well, and final absorbance was evaluated. The differences between final and initial absorbance readings were determined for samples and glucose standards. The glucose standard curve was used to calculate sample glycogen concentration (glucose equivalents, µmol/g wet weight). Using these methods, the change in absorbance of samples represents glucose released from glycogen as well as free glucose and G6P. Consequently, the glycogen value was later corrected by subtracting glucose and G6P concentrations, which were determined using a similar assay. Free glucose and G6P were extracted from powdered muscle diluted in 0.5 M perchloric acid (1: 10, w/v). Samples were homogenized and centrifuged, and supernatants were plated in triplicate on 96 well plates. Assay media was added to each well (final concentration: 400 mM triethanolamine, 28 mM EDTA, 40 mM $MgCl_2$, 2 mM NADP and 1.2 mM ATP, pH adjusted to 7.6). Initial absorbance was read at 340 nm. The assay was performed with sequential additions of G6PDH (2 U/well) and HK (2.1 U/well). The change in absorbance after each addition represents G6P and free glucose, respectively. Sample G6P and glucose concentrations were calculated using standard curves as described for glycogen.

Lactate analysis was conducted using the same homogenate as described by glucose and G6P analysis. Samples were plated in triplicate and assay media was added (final concentration: 430 mM glycine, 1.2% hydrazine, pH 9; 2.5 mM NAD). After the initial absorbance reading at 340 nm, lactate dehydrogenase (bovine heart LDH; Sigma, St. Louis, MO) was added (2 U/well), and the plate was incubated on a rocker at room temperature for 3 h. Lactate concentrations of samples were calculated using a standard curve.

Concentration of ATP was originally described by Passonneau and Lowry (1993) and adapted to a 96-well plate by Copenhafer et al. (2006). In brief, muscle samples were extracted using 0.5 M perchloric acid as previously described, however the supernatant was neutralized using 2 M KOH. If necessary, the pH was adjusted to 6.5 – 8.0. After precipitating on ice for 10 min, microtubes were centrifuged at $13,000 \times g$ for 5 min. Supernatant was transferred to a new tube and stored at −80°C until analysis. The standards and samples were mixed with assay media (350 mM triethanolamine, 25 mM EDTA, 35 mM $MgCl_2$, 0.5 mM ADP, 1.0 mM NADP, 0.1% BSA, and 10 µM P^1,P^5-di(adenosine-5')pentaphosphate, pH 7.6), glucose (0.9 mM), and 3.6 U of G6PDH in glass tubes. Samples were plated in triplicate (200 µl per well) and initial absorbance was read at 340 nm. The assay was performed with sequential additions of HK (7 U) and creatine kinase (30 U) to tubes. After each addition, samples were plated in triplicate; the additions correspond to ATP and phosphocreatine, respectively. Glycogen, G6P, glucose, lactate, and ATP concentrations are reported as µmol/g tissue (wet weight).

Electrophoresis and immunodetection

All samples (n = 36) were extracted and prepared as previously described by Ramos et al. (2020). After heating, samples were kept at −20°C until loaded into acrylamide gels. For calpain-1 and calpastatin identification, resolving gels with 7% acrylamide (37.5: 1 acrylamide: bis-acrylamide) were used, while 10% acrylamide gels were used for caspase-3 and 15% acrylamide gels for desmin and troponin-T. Stacking gels contained 5% acrylamide and were used for all gels. The amount of protein loaded for each respective gel was 5 µg (troponin-T), 10 µg (caspase-3 and desmin) and 15 µg (calpain-1 and calpastatin) per well and running times were adjusted according to protein sizes. Immediately after running, proteins were transferred to nitrocellulose membranes and dried overnight. The total protein stain (Revert, LI-COR, Lincoln, NE) was used to quantify and generate an index allowing content normalization and comparison across muscles. Membranes were blocked (Start Blocking TBS Blocking Buffer, Thermo Scientific, Rockford, IL) and then incubated with primary antibody diluted in blocking buffer with 0.2% Tween 20. Primary antibodies and dilutions were anti-troponin-T (T6277, Sigma, St. Louis, MO) 1: 20,000; anti-desmin (D1033, Sigma, St. Louis, MO) 1: 10,000; anti-procaspase-3 (9668, Cell Signaling, Danvers, MA) 1: 1,000; anti-calpain-1 (MA3-940, Thermo Scientific) 1: 10,000; and anti-calpastatin (MA3-944, Thermo Scientific) diluted 1: 5,000. Membranes were incubated with primary antibodies at 4°C overnight. Membranes were then washed 4 times (5 min each) with $1 \times$ TBS-0.1%

Tween 20, followed by 1 h incubation with specific dye-conjugated secondary antibody (IRDye 800 CW, LI-COR, Lincoln, NE) selected based on host from primaries and diluted 1: 10,000. After staining with the secondary antibody, membranes were washed as previously indicated, and then there was a final wash with $1 \times$ TBS (without Tween 20). Membranes were immediately scanned using an Odyssey CLx (LI-COR, Lincoln, NE), and quantified with Image Studio software version 5.2.

Quantification and final calculations were reported according to each protein. Procaspase-3 and calpastatin are reported as intact band signal (35 and 135 kDa, respectively). For calpain-1 the sum of signal from the 3 bands represented the total signal (calpain-1 total content), and the signal from the 76 kDa band was reported as a percentage of the total and labeled as complete autolysis. Desmin and troponin-T are reported as the disappearance of the intact band (54 and 37 kDa, respectively) representing their degradation. All proteins were reported as fold difference from LL at 1 h.

Statistical analysis

Experimental design was a complete randomized block, with block as slaughter dates. The model included the fixed effects of muscle, time postmortem, and their interaction. Normal distribution of residuals as well as variance homogeneity were tested, and data transformation was applied when needed. Time postmortem was considered as a repeated measure and least square means were separated by Bonferroni test at 5% significance, using SAS University Edition software.

Results and Discussion

Myosin heavy chain

The LL and Dia exhibited different MyHC isoform profiles (Figure 1), consistent with their function in the body. The LL, which extends the spine, contained a high proportion of type IIx MyHC (approximately 66%). In contrast, Dia contained approximately 80% type I and 20% type IIa MyHC, and type IIx MyHC was not detectable. This aligns with the Dia's role in respiration: a continuous, repetitive activity, which requires fatigue resistant fibers. Differences in MyHC composition were expected based on muscle function *in vivo* and confirmed that we had examples of a fast glycolytic muscle (LL) and a slow oxidative muscle (Dia).
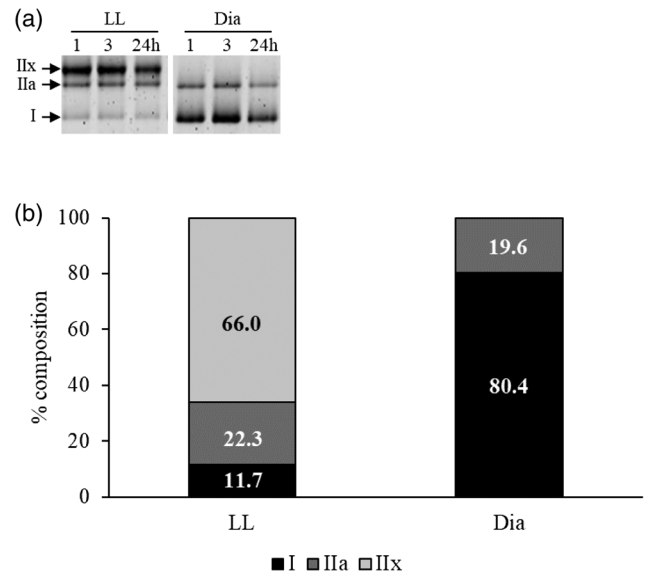

Figure 1. (A) Representative image of myosin heavy chain isoform separation by SDS-PAGE and (B) percent composition of myosin heavy chain isoforms in bovine LL and Dia. DIA, *diaphragm*; LL, *longissimus lumborum*; SDS-PAGE, sodium dodecyl sulfate polyacrylamide gel electrophoresis.

Substrate and metabolites

As expected, divergent MyHC isoform composition coincided with different patterns of postmortem metabolism. Ultimately, exsanguination requires greater dependence on anaerobic pathways for ATP production. Fast fibers generally contain more phosphocreatine (PCr) than slow fibers, which provides a more immediate source to generate ATP and protect against ATP disappearance (Schiaffino and Reggiani, 2011). We detected PCr in LL 1 h postmortem but could not detect PCr in Dia (data not shown). Postmortem ATP concentration was influenced by muscle ($P < 0.01$) and time ($P < 0.01$; Figure 2). Initial ATP contents were greater in LL, which may be related to fiber type differences: glycolytic muscles generally have higher resting concentrations of ATP (Kushmerick et al., 1992) and greater PCr to provide a temporal buffer against energy loss (Egan and Zierath, 2013).

Furthermore, fast fibers are more well-suited for anaerobic glycolysis due to greater content of glycolytic enzymes, along with higher amounts of substrate glycogen (Figure 3A). Glycogen degradation differed according to muscle type during the postmortem period (m × t: $P < 0.01$). While glycogen decreased in the LL ($P < 0.01$) and Dia ($P = 0.05$) from 1 to 24 h, the change in glycogen content in the LL was more pronounced compared to Dia. The initial (1 h) glycogen content was higher in the LL compared to the Dia ($P = 0.09$). Higher glycogen content in the LL is
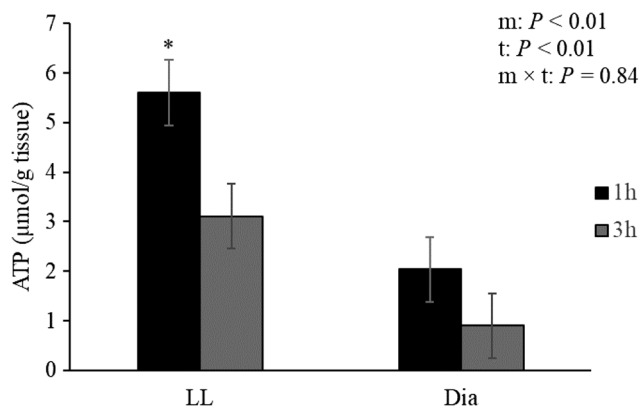
Figure 2. Early postmortem (1 and 3 h) ATP concentration (μmol/g tissue) in bovine LL and Dia. *Indicates difference ($P < 0.05$) between muscles within time postmortem. ATP, adenosine triphosphate; DIA, *diaphragm*; LL, *longissimus lumborum*. m = muscle, t = time

consistent with its greater proportion of fast, type IIx MyHC. Glycogen degradation postmortem is due to the concerted action of phosphorylase and glycogen debranching enzyme, the latter enzyme being responsible for accumulation of free glucose (Matarneh et al., 2017). In accord, both muscle ($P < 0.01$) and time ($P < 0.01$) affected muscle glucose concentration (Figure 3B). Glucose increased in both LL ($P < 0.01$) and Dia ($P < 0.01$) and was greater ($P < 0.05$) in LL than Dia at 3 and 24 h postmortem. Glucose-6-phosphate is generated as a result of glycogen phosphorylase activity and subsequent isomerization of glucose-1-phosphate to G6P. At later times postmortem, G6P may accumulate due to inactivation of phosphofructokinase (England et al., 2014; Scheffler and Gerrard, 2007). Glucose-6-phosphate content was also affected by muscle ($P < 0.01$) and time ($P < 0.01$; Figure 3C), increasing within LL ($P < 0.01$) and Dia ($P < 0.01$) during the postmortem period. In the LL, G6P was similar at 1 and 3 h, but increased by 24 h ($P < 0.01$). Compared with Dia, the LL had higher G6P content at 1 and 24 h ($P < 0.01$), but similar at 3 h postmortem.

Lactate, the final product of anaerobic glycolysis, changed more markedly in the LL than in the Dia (m × t: $P < 0.01$; Figure 3D). Within each muscle, lactate increased postmortem ($P \leq 0.05$). However, lactate production after 3 h was limited in the Dia (~7 μmol/ g tissue; $P = 0.12$), whereas lactate increased in the LL (~30 μmol/g tissue; $P < 0.01$). Lactate was similar in the LL and Dia at 1 h postmortem ($P = 0.24$), suggesting that anaerobic glycolysis was more effective at maintaining greater ATP level in the LL compared to the Dia. At 3 h, lactate tended to differ between
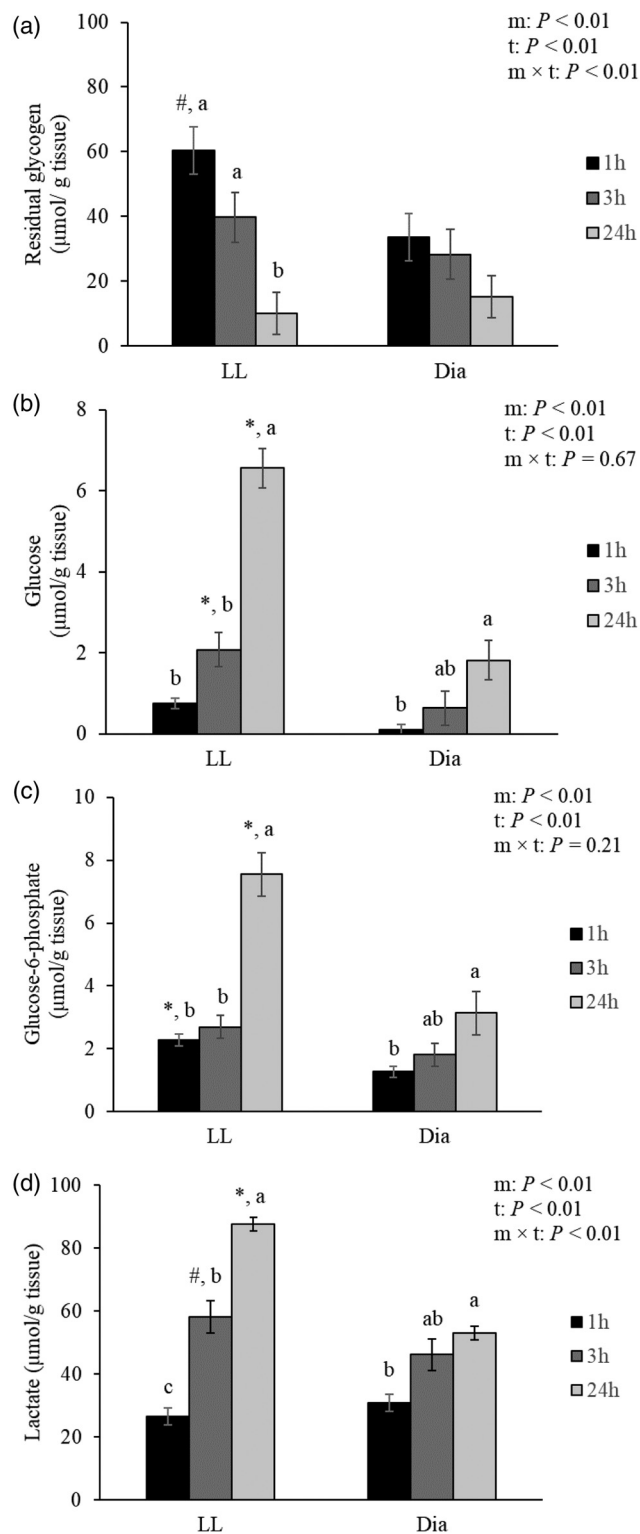
Figure 3. (A) Residual glycogen, (B) glucose, (C) G6P, and (D) lactate concentrations (μmol/g tissue) in bovine LL and Dia. #Indicates trend ($P < 0.10$) and *indicates difference ($P < 0.05$) between muscles within time postmortem; [a,b,c]Indicates difference ($P < 0.05$) between time postmortem within muscle. DIA, *diaphragm*; G6P, glucose 6-phosphate; LL, *longissimus lumborum*. m = muscle, t = time

muscles ($P = 0.09$), but by 24 h, muscle lactate content was higher in LL ($P < 0.01$).

Protease content postmortem

As a zymogen, caspase must be cleaved to be converted into an active enzyme. Although the antibody used was selected based on its ability to detect both intact and cleaved caspase-3 bands, only the intact procaspase-3 (35 kDa band) was detected in both muscles during the first 24 h postmortem (Figure 4A). The muscles showed different ($P < 0.01$) procaspase-3 content, with the Dia having more than double the content compared to the LL at 1 h (Figure 4B). The conversion of inactive procaspase-3 into an active enzyme would represent a decrease in the intact band and formation of bands with lower molecular weights. However, during time postmortem the content was similar ($P = 0.42$) between and within muscles. Previously, we investigated caspase-3 content and activation in LL with contrasting tenderization up to 14d postmortem, with no detectable cleaved band and greater content associated with faster tenderizing beef (Ramos et al., 2020). This association and the evidence that caspase-3 is associated with calpastatin cleavage in an *in vitro* study (Huang et al., 2014) enforces the idea that caspase-3 could synergistically act with calpain to overcome the inhibitory activity of calpastatin. Earlier calpastatin breakdown would relieve its inhibition of calpain, thereby promoting calpain activity as time postmortem progresses. If the caspase-dependent cell death pathway was in place, the procaspase-3 content should decrease over time, representing its activation and positive contribution to tenderization; however, this was not the case.

The mechanism by which skeletal muscle cells die during the muscle to meat conversion continues to be subject to debate. For example, it was proposed that the sudden decrease in cyclic AMP after slaughter would inactivate protein kinase A, with consequent inhibition of the phosphorylation of heat shock protein beta 6 (HSPB6; Longo et al., 2015). According with authors, unphosphorylated HSPB6 is able to interact with Bax enhancing apoptosis through caspase-3 activation. However, the time frame for the observed changes in the disappearance of unphosphorylated HSPB6 was from 1 up to 17d postmortem, much longer than the time frame of present study. On the other hand, the release of cytochrome *c* from the mitochondrial inter-membrane space to the cytosol was proposed to be the central step preceding caspase-3 activation and apoptosis initiation; this event took place between 6 and 12 h postmortem in bovine *longissimus dorsi* (Zhang et al., 2017). Using a more sensitive approach, we previously demonstrated that the outer membrane is permeabilized and cytochrome *c* may be released sometime between 1 and 3 h postmortem, with faster progress in LL compared to Dia (Ramos et al., 2021). The release of cytochrome *c* is also present in caspase-independent cell death, with at least 12 types of programmed cell death, not including the possible transition between types (Yan et al., 2020). Due to these findings, the mechanism involved in the conversion of muscle to meat that is concomitant with protease activation must be further investigated. It is also important to consider recent evidence regarding the importance of mitochondrial calcium handling, including its role as a regulator of permeability transition pore opening, reactive oxygen species production, and induction of cell death by necroptosis involving mito-dysfunction (Faizan and Ahmad, 2021). Proteolysis mediated tenderization of beef is largely driven by calpain, which is calcium-dependent (Koohmaraie, 1992a). Calcium handling dynamics between the sarcoplasmic reticulum, mitochondria, and sarcoplasm can directly influence proteolysis.
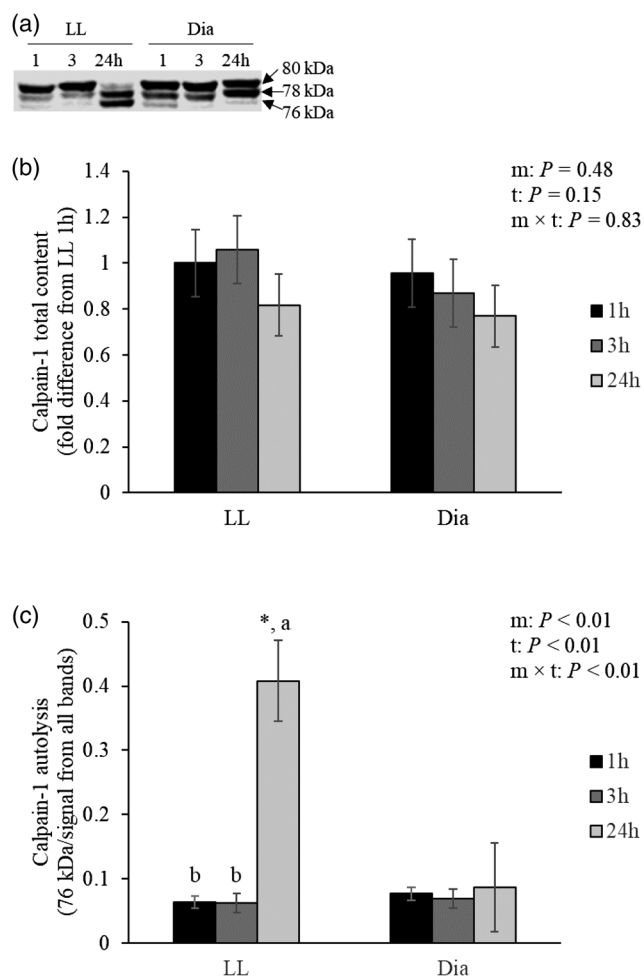
Calpain-1 activation and autolysis are a two-step process. The first step is represented by the cleavage of the catalytic subunit (80 kDa band) and formation of the intermediate product (78 kDa band); this is followed by a second cleavage, resulting in the formation of the 76 kDa autolytic fragment (Goll et al., 2003). In both muscles 3 distinct bands were identified (Figure 5A). Total calpain-1 content was similar between
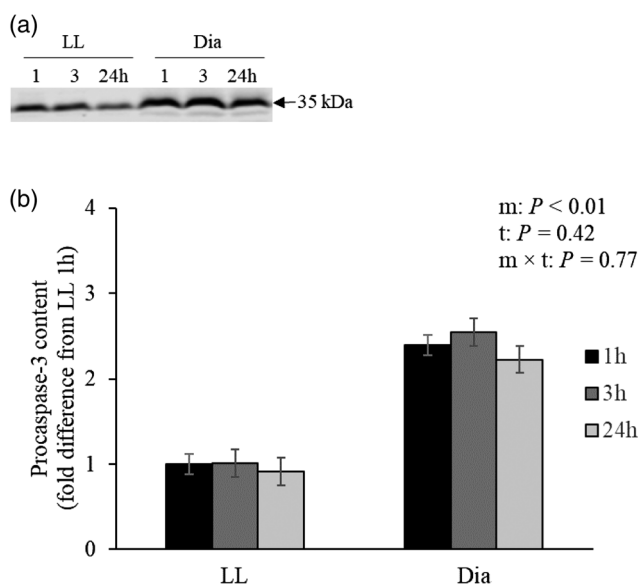
Figure 4. (A) Procaspase-3 identification by immunodetection; and (B) relative procaspase-3 content in bovine LL and Dia at 1, 3, and 24 h postmortem. DIA, *diaphragm*; LL, *longissimus lumborum*. m = muscle, t = time

muscles (Figure 5B). However, calpain-1 autolysis differed between the muscles during the first 24 h postmortem (m × t: $P < 0.01$; Figure 5C). The LL showed greater and earlier autolysis when compared to Dia, with difference evident at 24 h postmortem. In the Dia, the autolyzed fragment was barely present throughout the 24 h period. However, in the LL, there was a prominent increase in the autolyzed fragment from 3 to 24 h postmortem.

The progression of calpain-1 activation and autolysis is governed by calpastatin (Goll et al., 2003; Koohmaraie, 1992b). The intact band representing calpastatin (135 kDa band) was identified in both muscles throughout the period (Figure 6A). However, in accordance with the abrupt increase in the progression of the calpain-1 autolysis, the band representing the intact calpastatin in the LL decreased from 3 to 24 h postmortem

(m × t: $P < 0.01$; Figure 6B). Similar to the difference in procaspase-3 content between muscles, the Dia showed more than 2-fold calpastatin content than in the LL. However, in the present study and contrary to the findings by Huang et al. (2014), greater procaspase-3 content does not seem to be associated with an accelerated cleavage of calpastatin, which cleaved faster in the LL muscle. Additionally, greater calpastatin content and limited progression of calpain-1 activation represents an impairment to proteolysis.

Proteolysis of desmin and troponin-T

The degradation of the intermediate filament, desmin, was evaluated based on the disappearance of its intact band (54 kDa band; Figure 7A). Intact desmin was similar during the postmortem period (t; $P = 0.13$), however content differed between muscles ($P < 0.01$; Figure 7B). The Dia had approximately 50% greater desmin than the LL. Intact desmin was similar throughout the 24 h period in the Dia ($P = 0.65$). On the other hand, in the LL the intact band decreased from 1 and 3 h compared to 24 h ($P = 0.02$), as evidenced by the contrast. Therefore, desmin
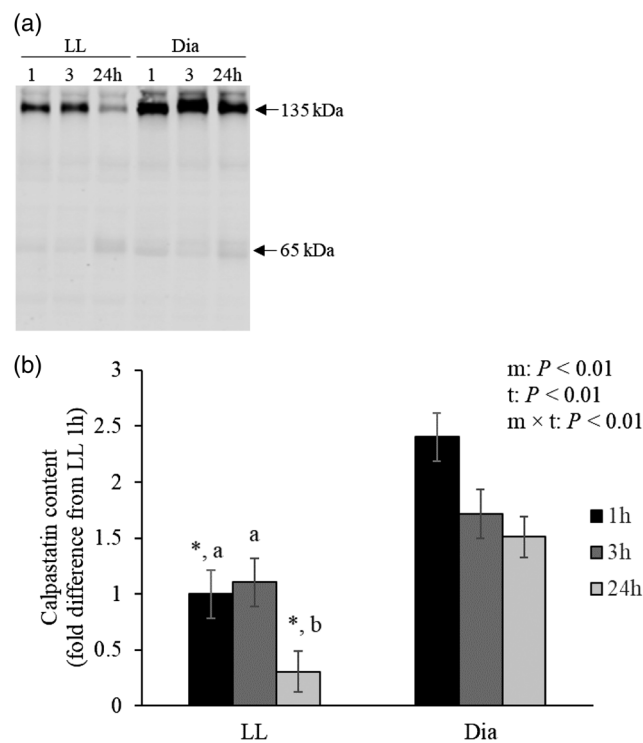

Figure 5. (A) Calpain-1 identification by immunodetection; (B) relative calpain-1 total content; and (C) autolysis (76 kDa) in bovine LL and Dia at 1, 3, and 24 h postmortem. *Indicates difference ($P < 0.05$) between muscles within time postmortem; [a,b,c]Indicates difference ($P < 0.05$) between time postmortem within muscle. DIA, *diaphragm*; LL, *longissimus lumborum*. m = muscle, t = time
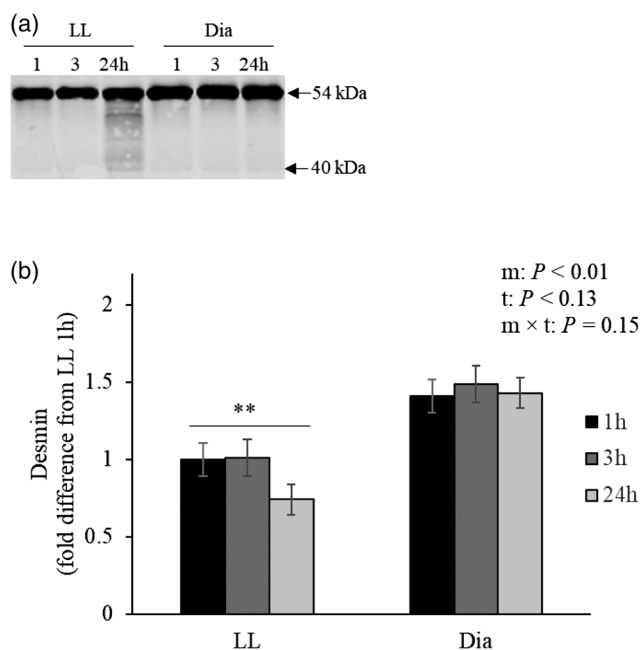
Figure 6. (A) Calpastatin identification by immunodetection; and (B) relative content of intact calpastatin in bovine LL and Dia at 1, 3, and 24 h postmortem. *Indicates difference ($P < 0.05$) between muscles within time postmortem; [a,b,c]Indicates difference ($P < 0.05$) between time postmortem within muscle. DIA, *diaphragm*; LL, *longissimus lumborum*. m = muscle, t = time

was degraded in the LL during the 24 h postmortem period in agreement with calpain-1 activation and autolysis.

Troponin-T degradation was also investigated as the disappearance of its intact band ($\sim$ 37 kDa band; Figure 8A). Once again, the muscles differed ($P <$ 0.01), with troponin-T content being greater in the LL than in the Dia (Figure 8B). Early time postmortem did not affect troponin-T disappearance. However, bands representing the troponin-T degradation product were observed in the LL at 24 h (Figure 8A). This evidence is consistent with greater calpain-1 activation, less intact calpastatin remaining at 24 h postmortem, and desmin degradation.

The specialized function of muscle fibers is reflected in the expression profile of proteins and isoforms. In skeletal muscle, the intermediate filament, desmin, is partly responsible for the maintenance of the muscle fiber's structure: it connects adjacent myofibrils and links myofibrils with the sarcolemma, and positions mitochondria (Paulin and Li, 2004). As Dia has a greater proportion of MyHC isoform type I and greater mitochondrial content, it also has increased desmin content. On the other hand, troponin-T helps anchor the troponin complex to the thin filament, organizes the complex, and modulates contraction and relaxation (reviewed by Wei and Jin, 2011).

Figure 7. (A) Desmin degradation shown by immunodetection; and (B) relative content of intact desmin (54 kDa) in bovine LL and Dia at 1, 3, and 24 h postmortem. **Indicates difference ($P < 0.01$) between muscles within time postmortem. DIA, *diaphragm*; LL, *longissimus lumborum*. m = muscle, t = time
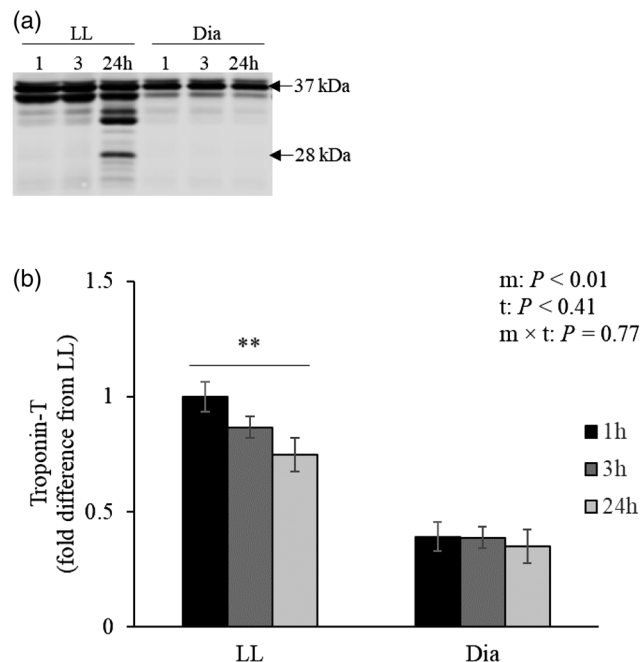
Figure 8. (A) Troponin-T degradation shown by immunodetection; and (B) relative content of intact troponin-T (37 kDa) in bovine LL and Dia at 1, 3, and 24 h postmortem. **Indicates difference ($P < 0.01$) between muscles within time postmortem. DIA, *diaphragm;* LL, *longissimus lumborum*. m = muscle, t = time

Additionally, troponin-T has specific isoforms related to fiber types, with exclusive expression of a slow isoform in type I fibers in adult animals (Wei and Jin, 2011) and pigs (Muroya et al., 2010). These isoforms exhibit different susceptibility to proteolysis, with the degradation of fast troponin-T progressing more rapidly in type IIb fibers than in type I fibers, along with desmin (Muroya et al., 2010). Our results agree that both proteins are degraded faster in LL (mostly glycolytic) compared to Dia (mostly oxidative), although we investigated protein degradation in muscle homogenate rather than in single fibers.

Conclusion

The glycolytic LL muscle was associated with faster calpain-1 autolysis and, therefore, the start of proteolysis. However, it was not possible to detect activation of caspase-3 in the LL nor the Dia, and the disappearance of intact calpastatin at 24 h postmortem was not associated with greater content of procaspase-3. However, the absence of caspase-3 activation does not undermine the contribution of aerobic metabolism in early postmortem period in either muscle. The relationship between greater mitochondrial content and the delayed protease activation points to the importance of calcium in oxidative

muscle. The Dia muscle showed greater content of calpastatin and reduced proteolysis, which may be partly due to capacity of Dia to limit increases in sarcoplasmic calcium earlier postmortem. On the other hand, early decline in ATP and glycogen concentrations were associated with the reduced mitochondrial content and contribution in the LL, as well as a greater calpain-1 activation, and start of proteolysis.

Acknowledgments

Literature Cited

Bergmeyer, H. U. 1974. Methods of enzymatic analysis. New York: Academic Press.

Charles, A.-L., A.-S. Gilbert, M. Guillot, S. Talha, A. Lejay, A. Meyer, M. Kindo, V. Wolff, J. Bouitbir, J. Zoll, and B. Geny. 2017. Muscles susceptibility to ischemia-reperfusion injuries depends on fiber type specific antioxidant level. Front. Physiol. 8:52. https://doi.org/10.3389/fphys.2017.00052

Copenhafer, T. L., B. T. Richert, A. P. Schinckel, A. L. Grant, and D. E. Gerrard. 2006. Augmented postmortem glycolysis does not occur early postmortem in AMPKγ3-mutated porcine muscle of halothane positive pigs. Meat Sci. 73:590–599. https://doi.org/10.1016/j.meatsci.2006.02.015

Dang, D. S., J. F. Buhler, H. T. Davis, K. J. Thornton, T. L. Scheffler, and S. K. Matarneh. 2020. Inhibition of mitochondrial calcium uniporter enhances postmortem proteolysis and tenderness in beef cattle. Meat Sci. 162:108039. https://doi.org/10.1016/j.meatsci.2019.108039

Delgado, E. F., G. H. Geesink, J. A. Marchello, D. E. Goll, and M. Koohmaraie. 2001a. Properties of myofibril-bound calpain activity in longissimus muscle of callipyge and normal sheep. J. Anim. Sci. 79:2097–2107.

Delgado, E. F., G. H. Geesink, J. A. Marchello, D. E. Goll, and M. Koohmaraie. 2001b. The calpain system in three muscles of normal and callipyge sheep. J. Anim. Sci. 79:398–412. https://doi.org/10.2527/2001.792398x

Egan, B., and J. R. Zierath. 2013. Exercise metabolism and the molecular regulation of skeletal muscle adaptation. Cell Metab. 17:162–184. https://doi.org/10.1016/j.cmet.2012.12.012

England, E. M., S. K. Matarneh, T. L. Scheffler, C. Wachet, and D. E. Gerrard. 2014. pH inactivation of phosphofructokinase arrests postmortem glycolysis. Meat Sci. 98:850–857. https://doi.org/10.1016/j.meatsci.2014.07.019

Faizan, M. I., and T. Ahmad. 2021. Altered mitochondrial calcium handling and cell death by necroptosis: An emerging paradigm. Mitochondrion 57:47–62. https://doi.org/10.1016/j.mito.2020.12.004

Geesink, G. H., S. Kuchay, A. H. Chishti, and M. Koohmaraie. 2006. μ-Calpain is essential for postmortem proteolysis of muscle proteins. J. Anim. Sci. 84:2834–2840. https://doi.org/10.2527/jas.2006-122

Geesink, G. H., and M. Koohmaraie. 1999. Effect of calpastatin on degradation of myofibrillar proteins by μ-calpain under postmortem conditions. J. Anim. Sci. 77:2685–2692. https://doi.org/10.2527/1999.77102685x

Goll, D. E., V. F. Thompson, H. Li, W. Wei, and J. Cong. 2003. The Calpain System. Physiol. Rev. 83:731–801. https://doi.org/10.1152/physrev.00029.2002

Goodman, C. A., D. M. Mabrey, J. W. Frey, M. H. Miu, E. K. Schmidt, P. Pierre, and T. A. Hornberger. 2011. Novel insights into the regulation of skeletal muscle protein synthesis as revealed by a new nonradioactive in vivo technique. FASEB J. 25:1028–1039. https://doi.org/10.1096/fj.10-168799

Huang, F., M. Huang, H. Zhang, B. Guo, D. Zhang, and G. Zhou. 2014. Cleavage of the calpain inhibitor, calpastatin, during postmortem ageing of beef skeletal muscle. Food Chem. 148:1–6. https://doi.org/10.1016/j.foodchem.2013.10.016

Koohmaraie, M., and G. H. Geesink. 2006. Contribution of postmortem muscle biochemistry to the delivery of consistent meat quality with particular focus on the calpain system. Meat Sci. 74:34–43. https://doi.org/10.1016/j.meatsci.2006.04.025

Koohmaraie, M. 1992a. The role of Ca2+-dependent protease (calpains) in post mortem proteolysis and meat tenderness. Biochimie 74:239–245.

Koohmaraie, M. 1992b. Effect of pH, temperature, and inhibitors on autolysis and catalytic activity of bovine skeletal muscle mu-calpain. J. Anim. Sci. 70:3071–3080.

Koohmaraie, M. 1996. Biochemical factors regulating the toughening and tenderization processes of meat. Meat Sci. 43 (suppl. 1):193–201. https://doi.org/10.1016/0309-1740(96)00065-4

Kushmerick, M. J., T. S. Moerland, and R. W. Wiseman. 1992. Mammalian skeletal muscle fibers distinguished by contents of phosphocreatine, ATP, and Pi. P. Natl. Acad. Sci. USA 89:7521–7525. https://doi.org/10.1073/pnas.89.16.7521

Longo, V., A. Lana, M. T. Bottero, and L. Zolla. 2015. Apoptosis in muscle-to-meat aging process: The omic witness. J. Proteomics 125:29–40. https://doi.org/10.1016/j.jprot.2015.04.023

Matarneh, S. K., E. M. England, T. L. Scheffler, and D. E. Gerrard. 2017. The conversion of muscle to meat. In: F. Toldra, editor, Lawrie's meat science. Woodhead Publishing. p. 159–185. https://doi.org/10.1016/B978-0-08-100694-8.00005-4

McMillan, E. M., and J. Quadrilatero. 2011. Differential apoptosis-related protein expression, mitochondrial properties, proteolytic enzyme activity, and DNA fragmentation between skeletal muscles. Am. J. Physiol.-Reg. I. 300:R531–R543. https://doi.org/10.1152/ajpregu.00488.2010

Muroya, S., P. Ertbjerg, L. Pomponio, and M. Christensen. 2010. Desmin and troponin T are degraded faster in type IIb muscle fibers than in type I fibers during postmortem aging of porcine muscle. Meat Sci. 86:764–769. https://doi.org/10.1016/j.meatsci.2010.06.019

Passonneau, J. V, and O. H. Lowry. 1993. Enzymatic analysis: A practical guide. Humana Press.

Paulin, D., and Z. Li. 2004. Desmin: a major intermediate filament protein essential for the structural integrity and function of muscle. Exp. Cell Res. 301:1–7. https://doi.org/10.1016/j.yexcr.2004.08.004

Ramos, P. M., L. C. Bell, S. E. Wohlgemuth, and T. L. Scheffler. 2021. Mitochondrial function in oxidative and glycolytic bovine skeletal muscle postmortem. Meat Muscle Biol. 5:1–16. https://doi.org/10.22175/mmb.11698

Ramos, P. M., S. A. Wright, E. F. Delgado, E. van Santen, D. D. Johnson, J. M. Scheffler, M. A. Elzo, C. C. Carr, and T. L. Scheffler. 2020. Resistance to pH decline and slower calpain-1 autolysis are associated with higher energy availability early postmortem in Bos taurus indicus cattle. Meat Sci. 159:107925. https://doi.org/10.1016/j.meatsci.2019.107925

Scheffler, T. L., and D. E. Gerrard. 2007. Mechanisms controlling pork quality development: The biochemistry controlling postmortem energy metabolism. Meat Sci. 77:7–16. https://doi.org/10.1016/j.meatsci.2007.04.024

Scheffler, T. L, M. B. Leitner, and S. A. Wright. 2018. Technical note: Protocol for electrophoretic separation of bovine myosin heavy chain isoforms and comparison to immunohistochemistry analysis. J. Anim. Sci. 96:4306–4312. https://doi.org/10.1093/jas/sky283

Schiaffino, S., and C. Reggiani. 2011. Fiber types in mammalian skeletal muscle. Physiol. Rev. 91:1447–1531. https://doi.org/10.1152/physrev.00031.2010

Wei, B., and J.-P. Jin. 2011. Troponin T isoforms and posttranscriptional modifications: Evolution, regulation and function. Arch. Biochem. Biophys. 505:144–154. https://doi.org/10.1016/j.abb.2010.10.013

Whipple, G., and M. Koohmaraie. 1992. Effects of lamb age, muscle type, and 24-hour activity of endogenous proteinases on postmortem proteolysis. J. Anim. Sci. 70:798–804. https://doi.org/10.2527/1992.703798x

Wright, S. A., P. Ramos, D. D. Johnson, J. M. Scheffler, M. A. Elzo, R. G. Mateescu, A. L. Bass, C. C. Carr, and T. L. Scheffler. 2018. Brahman genetics influence muscle fiber properties, protein degradation, and tenderness in an Angus-Brahman multibreed herd. Meat Sci. 135:84–93. https://doi.org/10.1016/j.meatsci.2017.09.006

Yan, G., M. Elbadawi, and T. Efferth. 2020. Multiple cell death modalities and their key features (Review). World Academy of Sciences Journal 2:39–48. https://doi.org/10.3892/wasj.2020.40

Zhang, J., Q. Yu, L. Han, C. Chen, H. Li, and G. Han. 2017. Study on the apoptosis mediated by cytochrome c and factors that affect the activation of bovine longissimus muscle during postmortem aging. Apoptosis 22:777–785. https://doi.org/10.1007/s10495-017-1374-2